# 8 Nonlinear optical antennas

Hayk Harutyunyan[1], Giogio Volpe[2] and Lukas Novonty[1]

1. The Institute of Optics, University of Rochester, USA
2. ICFO-Institut de Ciencies Fotoniques, Spain

## 8.1 Introduction

The concept of nanoantennas has emerged in optics as an enabling technology for controlling the spatial distribution of light on subdiffraction length scales. Analogously to classical antenna design, the objective of optical antenna design is the optimization and control of the energy transfer between a localized source, acting as receiver or transmitter, and the free radiation field. Most of the implemented optical antenna designs operate in the linear regime that is, the radiation field and the polarization currents are linearly dependent on each other. When this linear dependence breaks down, however, new interesting phenomena arise, such as frequency conversion, switching, and modulation. Beyond the ability of mediating between localized and propagating fields, a nonlinear optical antennas provides the additional ability to control the interaction between the two. Figure 8.1 sketches an example where the nonlinear antenna converts the frequency of the incident radiation, thus shifting the frequency of a signal centered at $\omega_1$ by a predefined amount$\Delta\ \omega$ into a new frequency band centered at $\omega_2$. Here we review the basic properties of nonlinear antennas and then focus on the nonlinearities achievable in either single-particle systems or more complex coupled-particle systems. In practice, the use of nonlinear materials - either metals or dielectrics - in the design of optical antennas is a promising route towards the generation and control of optical information.

## 8.2 Design fundamentals

The study of nonlinear optical antennas is still in its infancy. The design principles are based on the well established field of nonlinear optics [352, 353] that has its origins in the early 1960s, when second-harmonic generation was first observed in a piezoelectric crystal [354]. Many textbooks have been written on nonlinear optics and most of the early studies focused on the nonlinear response of bulk materials and their surfaces. The surface-specific nonlinear response of materials, in particular, was extensively studied in the 1970s and 1980s and remains a very active field today [355]. In particular, the *reduced dimensionality* of nanoscale structures gives rise to nonlinear behaviors that are considerably

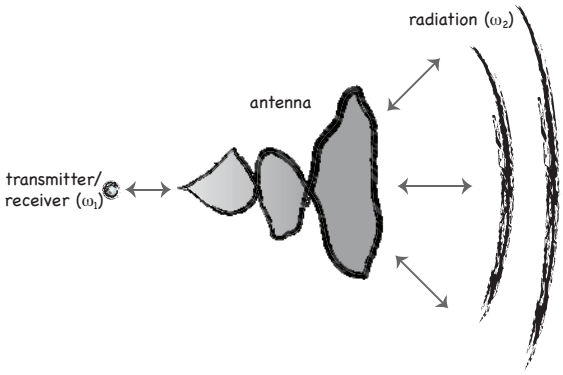


**Figure 8.1** Schematic of a nonlinear optical antenna. An optical antenna controls the energy transfer between a localized source, acting either as a transmitter or a receiver, and propagating light. Additionally, a nonlinear optical antenna also includes some abilities that arise when the linear regime breaks down, here the ability of frequency convert the incident radiation.

different from the bulk. For example, because of the inversion symmetry of a broad class of crystals, second-order effects cancel in the bulk and the nonlinear response of the material has its origin at the surface.

As the dimensionality of materials is reduced further, that is by going from bulk materials to nanowires or discrete particles, new phenomena arise. To this end, various authors studied roughened surfaces [356], randomly deposited particles on surfaces [357], or nanofabricated structures [358]. While interesting phenomena could be observed, the results were difficult to quantify, mainly because the samples were often either random and ill-defined or the response was averaged over many individual features. This led often to speculative conclusions about the physical origins of the observed nonlinear effects. However, the advent of nanoscience and nanotechnology made it possible to fabricate or synthesize samples with reduced dimensionality (nanostructures) in a systematic and controllable way, and to measure the nonlinear optical response from discrete and controllable structures [359, 360, 361, 202]. This level of control has paved the way to quantitatively measure the influence of individual physical parameters in the nonlinear processes, and to exploit the same nonlinear effects for novel optoelectronic applications.

### 8.2.1 Origin of optical nonlinearities in nanoantennas

Generally speaking, nonlinear optics exploits the nonlinear relationship between the exciting electric field $\vec{E}$ and resulting polarization $\vec{P}$. For weak excitation fields the relationship between $\vec{E}$ and $\vec{P}$ is linear, and most optical antennas operate in this regime. However, for strong excitations the response $\vec{P}$ depends on higher powers of $\vec{E}$, which gives rise to interesting and technologically important

phenomena, such as frequency mixing, rectification or self-phase modulation. The nonlinear relationship between $\vec{P}$ and $\vec{E}$ can be expressed as a series

$$\vec{P} = \epsilon_0 \left[ \chi^{(1)} \vec{E} + \chi^{(2)} \vec{E}\vec{E} + \chi^{(3)} \vec{E}\vec{E}\vec{E} + \ldots \right], \tag{8.1}$$

where the susceptibilities $\chi^{(n)}$ are tensors of rank $n+1$. The polarization $\vec{P}$ constitutes a secondary source current that, when inserted into Maxwell's equations, gives rise to a set of nonlinear differential equations.

Because the light-matter interaction is inherently weak it is often legitimate to approximate the response of a charged particle by a driven harmonic oscillator (Lorentz atom model). In this regime, the light-matter interaction is described by first-order perturbation theory. However, for strong excitation fields, such as those provided by pulsed lasers, first-order perturbation is no longer adequate, and the harmonic oscillator model has to be extended by including anharmonic terms. In such a less idealized model, therefore, the restoring force is no longer proportional to the displacement, as in the case of Hooke's law, but is rather nonlinear. While in the case of a harmonic oscillator the frequency of the oscillation is constant and defined by the parameters of the system, such as its mass and its spring constant, the oscillation frequency of the anharmonic oscillator turns out to depend on the amplitude of the driving field. Also, the energy stored at the fundamental frequency can now be coupled to and redistributed over other vibrational modes. For example, the inclusion of a quadratic anharmonic term in the equation of motion of the charge gives rise to solutions that oscillate not only at the fundamental frequency but also at the second harmonic, at the sum- and difference-frequencies. Similarly, by calculating the higher-order contributions or by including higher-order anharmonic terms in the functional form of the restoring force, one can generate third or higher order oscillations.

The charges oscillating at the new frequencies induce polarization currents $P(t)$, that gives rise to electromagnetic radiation at those new frequencies. In the simple example of second harmonic generation (SHG) under the driving field $E(t) = E\cos(\omega t)$, therefore, the induced nonlinear polarization will be

$$P^{(2)}(t) = \epsilon_0 \chi^{(2)} E^2(t) = 2\epsilon_0 \chi^{(2)} E^2 + 2\epsilon_0 \chi^{(2)} E^2 \cos(2\omega t)\ . \tag{8.2}$$

where, for simplicity, we assumed a nonlinear susceptibility that is constant in time (dispersion free). The first term describes rectification, that is the induced static field, and the second term is responsible for SHG. Similarly for the third order polarization, the same harmonic driving field leads to

$$P^{(3)}(t) = \epsilon_0 \chi^{(3)} E^3(t) = \frac{1}{4}\epsilon_0 \chi^{(3)} E^3 \cos(3\omega t) + \frac{3}{4}\epsilon_0 \chi^{(3)} E^3 \cos(\omega t), \tag{8.3}$$

where the first term describes third harmonic generation (THG) and the second one the Kerr nonlinearity, i.e. the change of the refractive index of the material at the fundamental frequency. As it will be discussed later, this effect can be used to tune the response of nanoantennas by changing the optical properties of the medium that they are embedded in.

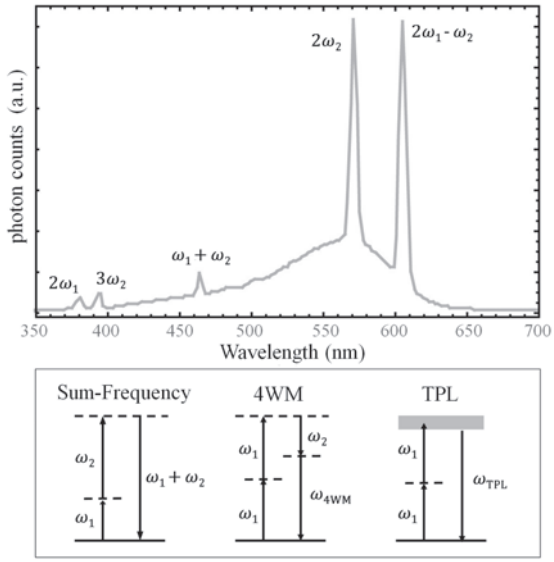


**Figure 8.2** Nonlinear response from a gold nanoantenna. Upper panel: typical spectrum obtained by irradiating the antenna with two infrared pulses of wavelengths 780 nm and 1140 nm. Sharp peaks, corresponding to different coherent nonlinear processes, can be observed on top of a broad incoherent TPL background. Lower panel: energy level description of different nonlinear processes, such as sum-frequency generation, singly degenerate four-wave mixing and two photon excited luminescence. The dashed lines indicate virtual excited states while the shaded area in the TPL scheme represents the continuum of interband states.

As shown in Fig. 8.2, when the driving field contains more than one discrete frequency, one observes a nonlinear response at mixing frequencies, such as sum- $(\omega_1 + \omega_2)$, difference- $(\omega_1 - \omega_2)$, or four-wave-mixing $(\omega_1 \pm \omega_2 \pm \omega_3)$. Another class of nonlinear processes involves a sequence of distinct optical interactions, such as the absorption of two photons followed by the emission of one photon, a process referred to as two-photon excited luminescence (TPL) (see Fig. 8.2). Because of its quadratic intensity dependence TPL is a very powerful tool to study local fields near metal nanoantennas [360]). Interestingly, TPL is a third-order nonlinear process. It can be understood by considering the average rate of energy dissipation in a polarizable material, which is according to Poynting's theorem

$$P_{\text{abs}} = -\int_V \left\langle \vec{j}(\vec{r},t) \cdot \vec{E}(\vec{r},t) \right\rangle \mathrm{d}V \ , \tag{8.4}$$

where $\langle .. \rangle$ denotes the time average and $\vec{j} = \mathrm{d}\vec{P}/\mathrm{d}t$ is the polarization current density. If we consider again a time-harmonic field $\vec{E}(\vec{r},t) = \mathrm{Re}\left[\vec{E}(\vec{r},\omega\,)\,\exp(-\mathrm{i}\omega t)\right]$, the time-average in Eq. (8.4) implies that $P_{\text{abs}}$ is non-zero only if $\vec{j}$ and $\vec{E}$ oscillate

at the same frequency. Thus, we can rewrite Eq. (8.4) as

$$P_{\text{abs}} = -\frac{1}{2}\int_V \text{Re}\left[\vec{j}(\vec{r},\omega\,)\cdot\vec{E}^*(\vec{r},\omega\,)\right]\,\text{d}V\ . \tag{8.5}$$

The lowest-order term in Eq. (8.1) that contributes to $P_{\text{abs}}$ is associated with $\chi^{(1)}$ and is responsible for linear absorption

$$P^{(1)}_{\text{abs}} = \frac{\omega}{2}\int_V \text{Im}\left[\chi^{(1)}(\omega)\right]\vec{E}\,\vec{E}^*\,\text{d}V\ , \tag{8.6}$$

where the argument $(\vec{r},\omega\,)$ has been omitted for brevity. The second order polarizability associated with $\chi^{(2)}$ oscillates at $2\,\omega$ and zero-frequency, hence there is no contribution to $P_{\text{abs}}$. The next higher contributing term is associated with $\chi^{(3)}$, and is responsible for two-photon absorption

$$P^{(3)}_{\text{abs}} = \frac{\omega}{2}\int_V \text{Im}\left[\chi^{(3)}(\omega,-\omega,\omega\,)\right]\vec{E}\,\vec{E}^*\,\vec{E}\,\vec{E}^*\,dV\ . \tag{8.7}$$

For an extended isotropic material irradiated by a plane wave this reduces to

$$P^{(3)}_{\text{abs}} \propto \text{Im}\left[\chi^{(3)}\right]\left|\vec{E}\right|^4\ , \tag{8.8}$$

featuring a quadratic intensity dependence on the intensity that is characteristic for two-photon absorption. Although the efficiency of TPL depends quadratically on the excitation power, the process is governed by a third-order nonlinear susceptibility. It is evident from the discussion that absorption is associated only with odd orders of $\chi$.

### 8.2.2 Nonlinear susceptibilities of optical materials

For the case of an atomic system, the values of $\chi^{(n)}$ can be estimated from the simple anharmonic oscillator model discussed before [353]. By using the values of the electron mass and charge, and by assuming that the electron displacement is on the order of atomic dimensions, one can estimate the second and third order susceptibilities to be $\chi^{(2)} = 7\times10^{-12}$ m/V and $\chi^{(3)} = 3.5\times10^{-22}$ m$^2$/V$^2$, values in good agreement with experimental parameters measured for non-resonant materials.

Because the nonlinear optical susceptibilities are very small there is a small chance of nonlinear frequency conversion when light interacts with a single atom. To improve the nonlinear conversion efficiency, traditional experiments use crystals many wavelengths in size. Nonlinear crystals not only increase the interaction volume, but they are designed to coherently enhance the nonlinear response through a process referred to as phase matching. In nanomaterials phase matching is not possible because the characteristic dimensions are smaller than the wavelength of light. The nonlinear conversion efficiency on the nanoscale can be resonantly enhanced by localized surface plasmons. For example, while the nonlinearity of bulk gold is defined by the intrinsic susceptibility $\chi^{(3)} = 7.6\times10^{-19}$

$m^2/V^2$, the third-order nonlinear response of gold nanoparticles embedded in glass can be enhanced up to 3 orders of magnitude [353].

Moreover, the susceptibilities also account for the crystal symmetry of materials. A driving field along one axis can generate a nonlinear polarization along a different axis. These symmetry properties are encoded in the susceptibility tensor. For example, the second order susceptibility $\chi^{(2)}$ has 9 elements and $\chi^{(3)}$ has 81 elements. Due to the symmetry of the crystal the number of independent tensor elements often reduces significantly, i.e. for a centrosymmetric crystal $\chi^{(3)}$ has only three independent tensor components. For small structures, such as optical antennas the nonlocal response near material boundaries provides additional degrees of freedom to control the nonlinear response. Thus, where the size is much smaller than the wavelength of the driving field not only the symmetry of the lattice is important, but also the overall shape of the nanostructures.

## 8.3 Nonlinearities in single nanoparticles

Single nanoparticles are the simplest examples of optical antennas. The nonlinear response of single nanoparticles is, therefore, a good case study. On the nanoscale, nonlinear optical phenomena are influenced by different factors, such as the symmetry of the crystal lattice and the symmetry of the particle shape.

### 8.3.1 Nanoscale and macroscale nonlinear phenomena

One of the most remarkable properties of metals at optical frequencies is their ability to support collective oscillations of surface charges (plasmons). In the case of plane metallic surfaces, these surface-bound modes possess a very distinct dispersion curve. Reducing the sample size to dimensions much smaller than the wavelength of light, such as in nanowires or nanoparticles, gives rise to resonances, called localized surface plasmons (LSP), that are defined by the size and shape of the sample, and that dominate the linear optical properties [362, 41]. Similarly, the nonlinear properties of metal particles at optical frequencies are also strongly influenced by their LSP resonances. Thus, unless symmetry constraints are involved, the resonances underlying the nonlinear processes follow those of the linear scattering processes. This correlation has, for example, been demonstrated using TPL from gold nanorods: changing the rod aspect ratio, in fact, not only shifts the plasmon resonance peak, but also tunes its luminescence [363]. Another remarkable feature of LSPs is their ability to facilitate electronic transitions that are forbidden in the bulk due to the momentum mismatch. For example, intraband transitions in gold have large wave vector and cannot be coupled to photons directly. However, due to their localized nature LSPs have flat dispersion and can possess arbitrarily large momenta. Thus the emission spectrum of gold nanoparticles features not only a visible TPL band,

as in the case of smooth gold films, but also one-photon induced luminescence in the near-infrared mediated by LSPs [360].

At optical frequencies, LSP resonances are commonly employed for enhancing the radiation from a local light source, such as a single molecule or quantum dot [75, 76, 364]. Here, the spectral profile of the emission resonance is typically altered according to the plasmonic resonance of the nanoparticle [244] or, in case of nonresonant enhancement, remains unchanged [365]. In the case of nonlinear processes, however, the coupling between the local source and the nanoantenna shows a different behavior. The nonlinear interaction between near-fields of the nanoparticle and a single molecule, for example, gives rise to spectral shifts in the SHG spectra, even in the case of non-resonant enhancement [366].

Unlike for bulk crystals, there is no phase matching for structures with sizes much smaller than a wavelength. Phase matching refers to the coherent superposition of the nonlinear response: a light which propagates through a nonlinear crystal, generates a nonlinear signal at each spatial point along its propagation path. To enhance the output of the signal, it is necessary to match the propagation speeds (match the phases) of the pump and signal beams along their path, so that all nonlinearly generated photons can interfere constructively. This is usually achieved by employing birefringent nonlinear crystals, where the refractive index depends on the polarization and the direction of the light that passes through. In a typical nonlinear generation scheme, the polarizations of the fields and the orientation of the crystal are chosen such that the phase-matching condition is fulfilled. As the size of the crystal becomes smaller, so does the optical path length. In the limit of crystals that are smaller than the wavelength of light it is no longer possible to generate constructive interference of the nonlinear response.

### 8.3.2 Symmetry considerations on the nanoscale

In bulk materials, the crystal symmetry defines the existence of certain nonlinear processes. The same is true for nanoscale materials, but the symmetry of the particle geometry also comes into play. For example, in order to achieve efficient SHG, an asymmetry is required in the motion of the electrons. For bulk crystals, this asymmetry is associated with the unit cell of the crystal's atomic structure, but in the case of nanostructures one can also exploit particle shapes lacking point symmetry. In fact an asymmetric nanoparticle can efficiently frequency double the incident field, even though the material has a symmetric lattice [359]. However, second harmonic generation is even possible for symmetric particle shapes and symmetric lattices. In this case, the nonlinear process is driven by higher-order multipolar modes. It has been shown theoretically [367, 368, 369, 370] and experimentally [371] that, in the simple case of a spherical particle illuminated by a plane wave, the scattered light at the second-harmonic frequency originates from a nonlocally excited electric dipole and a locally excited electric quadrupole terms.

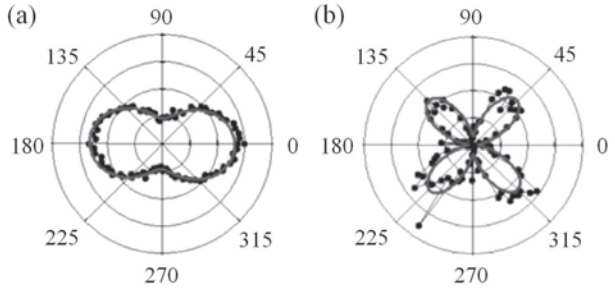


**Figure 8.3** SHG intensity polarized vertically with the respect to the scattering plane as a function of polarization angle of the excitation field for planar interface (a) and single gold nanoparticle (b). (Adapted with permission from Ref. [372]. Copyright (2010). American Chemical Society).

Thus, the angular distribution of nonlinearly scattered light can be different from the angular distribution of linearly scattered light. In general, the excitation of different multipolar modes depends on the symmetry of both the particle shape and the excitation beam [373]. In fact, the symmetry of the excitation beam can be used to filter out certain nonlinear processes. For example a circularly polarized excitation beam can be employed to suppress third-harmonic generation from axially symmetric particles [353]. This property can be used in selective imaging schemes to highlight nonsymmetric features [374].

### 8.3.3 Nonlinear polarization in nanoparticles

The polarization and the angular distribution of the radiated power depends on factors that are directly associated with LSP resonances of metal nanoparticles. The polarization of the emitted radiation depends on the nonlinear susceptibility tensor of the material and on the geometrical shape of the nanoparticles. It has been shown that the SH radiation from a plane interface exhibits a dipolar polarization distribution (see Fig. 8.3a), whereas the SH polarization from a single nanoparticle features a four lobe pattern, characteristic of a quadrupolar mode (see Fig. 8.3b) [372]. The contribution from even higher order modes, such as octupoles, have been observed in similar experiments [375]. The interference between different modes can be used to determine the relative contributions of surface and bulk nonlinearities [376].

Polarization effects can also be observed for incoherent nonlinear processes, such as TPL. For a single nanorod antenna geometry, the degree of polarization can be as low as zero for some metals (gold), while other metals (aluminum, silver) largely preserve the incoming polarization state [377]. The reason is that depending on the dimensions and the material of the particle, longitudinal and transversal plasmonic modes can be tuned in and out of resonance, thus giving rise to different degrees of polarization mixing.

## 8.4 Nonlinearities in coupled antennas and arrays

In many applications involving metal nanoparticles, an important role is played by their assemblies. Nowadays, it is clear that the optical plasmonic properties of a nanosystem strongly depend on the interplay between its constituting particles [378, 379]. In fact, coupled plasmonic oscillations take place whenever the near-field of a particle interacts with that of an adjacent particle [237]. The resonance of the coupled system occurs at a wavelength that is red-shifted from the resonance of an isolated particle, and the magnitude of this shift depends on the strength of the coupling between particles, which, in turn, depends on their proximity [378]. Interestingly, even though the absolute plasmon shift depends on many factors, such as the size and shape of the particles, the type of metal, and the surrounding medium, an independent universal scaling trend of the fractional shift of the wavelength$\Delta\ \lambda/\lambda_0$ can be observed when the distance $S$ between particles is scaled by their characteristic dimension $D$ [380, 381]

$$\frac{\Delta\lambda}{\lambda_0} = \frac{\lambda_1 - \lambda_0}{\lambda_0}\ \sim\ k\ \exp\left(-\frac{S}{\tau D}\right), \tag{8.9}$$

where $\lambda_1$ and $\lambda_0$ are the resonances of the coupled system and of the isolated particle respectively, $k$ is a fitting constant, and $\tau \approx 0.2$ for gold particles.

The coupling of the plasmonic oscillations can also lead to strong surface charge gradients at the separation gap between adjacent particles, thus dramatically enhancing their individual optical response by many orders of magnitude, as in the case of gap antennas [35, 204], and bowtie antennas [34].

These strong local fields have already found a variety of applications including sensing and trapping of objects on the nanometer scale [382, 383]. Moreover, such intense fields can substantially boost nonlinear optical processes, which typically scale with higher powers of the electric field. Coupled plasmonic particles have indeed been used to enhance the efficiency of various nonlinear optical processes, either in the metal itself or in media placed directly within a region of intense field enhancement. The employment of multiple elements and sophisticated antenna designs, therefore, provides even more tuning parameters for controlling the nonlinear response of nanomaterials. Further geometrical considerations, however, are very often necessary in order to design efficient frequency converters in the optical regime, where the coupling of many nanoparticles is concerned.

### 8.4.1 Enhancement of metal nonlinearities

The large field enhancement in coupled nanoantennas, such as bowtie antennas, and its dependence on the gap size have been successfully exploited to enhance different nonlinear processes of the metal, such as TPL, SHG, and THG [34, 384, 385]. As an additional degree of freedom, a more recent study showed that the tuning of the periodicity of an array of coupled nanoantennas can also be used to modulate both their linear and nonlinear optical properties [103].

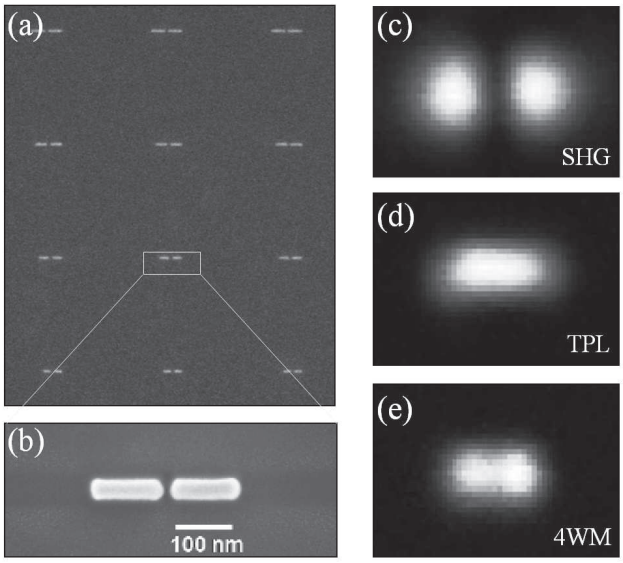


**Figure 8.4** Nonlinear response of gap antennas. (a) SEM micrography of an array of gold gap antennas fabricated by e-beam lithography and (b) close-up of a selected antenna. The antenna arms are 100nm-long nanorods separated by a gap of a few tens of nanometers. Confocal images of (c) SHG, (d) TPL, and (e) 4WM generated by a single antenna. The origin of the nonlinear signal is different in the three cases. The patterns in (c-e) reflect the symmetry of the nonlinear processes.

The enhancement of the metal nonlinearity as a function of the separation between coupled nanoparticles has been studied for the case of four-wave mixing (4WM) [202]: by decreasing the interparticle distance from large separation to touching contact, an increase of four orders of magnitudes of the 4WM signal can be achieved. This giant enhancement is associated with the shift of the LSP resonance, thus making one of the input wavelengths doubly resonant.

Among all the nonlinear processes, second harmonic generation is the most studied one. Although noble metals are centrosymmetric materials without a bulk SHG capability, it is still possible to generate SHG processes by exploiting symmetry breaking at metallic surfaces. Because of its quadratic intensity dependence, SHG can be increased by more than one order of magnitude at planar metal surfaces [386].

Symmetry considerations forbid SHG in centrosymmetric nanoparticle systems, even when asymmetric nanoparticles are arranged into patterns with inversion symmetry [387]. The coupling of particles with different sizes, however, can form a non-centrosymmetric system that can support SHG. This effect has been observed for an arrangement of asymmetric nanoparticles in a diffraction grating [388, 389], and, more recently, for arrays of T-shaped gold nanodimers [390].

Periodic subwavelength apertures can also be created on metal films in order

to further enhance SHG by many orders of magnitude. The first experimental demonstration of such an effect has been done by patterning a series of concentric surface grooves on a thin silver film, thus obtaining a increase in the frequency conversion efficiency due to an enhanced localized transmittance [391]. Similar SHG enhancement in metal films has been observed for other geometries, including overlapping double holes [392], periodic rectangular holes [393], and disordered aperture arrays [394].

Interestingly, experimental evidence indicates that multipole effects, such as magnetic dipoles and electric quadrupoles, can significantly contribute to the nonlinear emission of plasmonic nanosystems [395].

### 8.4.2 Enhancement of nonlinearities in surrounding media

Plasmonic structures can also enhance nonlinear effects by concentrating light into nonlinear media, such as gallium arsenide, placed directly within a region of field enhancement. In this case, the antenna concentrates optical radiation on a material that acts as a receiver. For example, the SHG efficiency of a nanopatterned isotropic GaAs substrate, located inside the subwavelength gaps of a metallic coaxial array, can be two orders of magnitude larger than that of a conventional nonlinear material, such as lithium niobate [396, 397].

Similarly, at room temperature, the spontaneous two-photon emission from AlGaAs can be enhanced by three orders of magnitude employing plasmonic nanoantenna arrays fabricated on the semiconductor surface [398].

High-harmonic generation has been recently observed in argon gas by exploiting the local field enhancement in the gap of gold bowtie antennas. With an enhancement exceeding 20 dB it was possible to generate high-harmonics up to the seventeenth order, which corresponds to an extreme ultraviolet wavelength of 47 nm [399].

Nonlinear antennas featuring a nonlinear material in the 'feedgap' region were theoretically discussed by [401, 402] and [59]. Zhou and coworkers derived an analytical model to show how the intensity-dependent refractive index of the nonlinear load can be used to tune the plasmonic resonance, giving rise to an optical bistability effect analogous to the classical bistability observed in Fabry-Perot resonators [401]. Chen and Alù have discussed the behavior of optically bistable antennas for applications, such as memories, switches and transistors [59]. In another recent study, a photoconductive load made of silicon has been proposed for ultrafast switching of the coupling of the nanoantenna elements from capacitive to conductive [402]. These calculations suggest that it is possible to achieve dramatic spectral shifts using very modest pumping energies, thus controlling both the near-field and the far-field of a nanoantenna. Similarly, a few works, both experimental [403] and theoretical [404, 405, 406], studied the bistability in metallic nanohole arrays embedded in nonlinear dielectric media.

Although the nonlinear processes in metal-dielectric compounds are ultimately related to the excitation of localized plasmons, the nonlinear response cannot al-

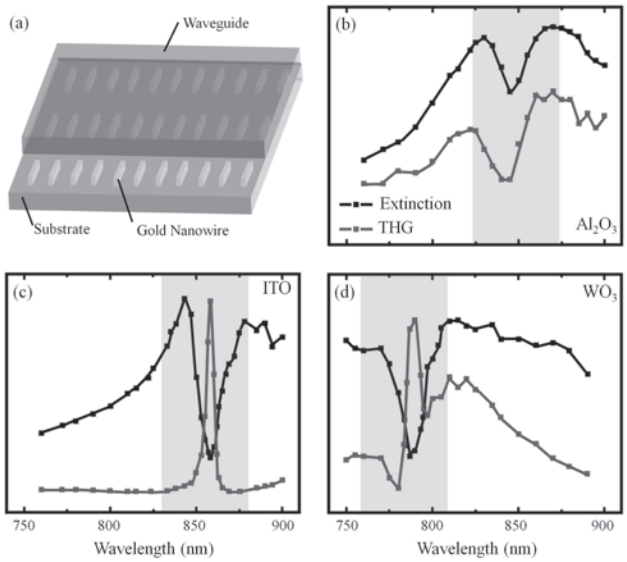


**Figure 8.5** Origin of the nonlinearity in plasmonic-dielectric hybrid systems. (a) Sketch of the metallic photonic crystal where a 1D gold nanowire grating is embedded between a quartz substrate and a dielectric slab waveguide of different materials. (b) Extinction and THG spectra of a sample featuring a low $\chi^{(3)}$ waveguide made of $Al_2O_3$. No THG peak is visible at the extinction dip; therefore, the metal contribution dominates. (c) For a high $\chi^{(3)}$ waveguide made of indium tin oxide (ITO), the nonlinear response of the waveguides dominates and lead to a strong THG peak at the extinction dip. (d) For a waveguide made of $WO_3$ (intermediate $\chi^{(3)}$) contribution from both metal and dielectric are observed. (Adapted with permission from Ref. [400]. Copyright (2011). Americal Physical Society).

ways be predicted from their linear optical response. In particular, the origin of the response can be concealed by the interplay of the nonlinear response of metal and the surrounding medium. For example, Utikal and colleagues demonstrated that the origin of the THG in hybrid plasmonic-dielectric compounds can be univocally identified from the shape of the nonlinear spectrum [400] (see Fig. 8.2). For coupled metal nanowires embedded in a dielectric waveguide, the strong coupling of the plasmonic modes gives rise to a sharp dip in the linear extinction spectrum. At the wavelength of the extinction dip, therefore, the electromagnetic fields are confined to the volume of the waveguide and not to the plasmonic modes. Thus by changing the nonlinearity of the waveguide, from low (see Fig. 8.5b) to high (see Fig. 8.5c), one can tune the nonlinear spectral response of the structure while preserving its linear response.

### 8.4.3 TPL nonlinear microscopy of coupled particles

The use of TPL as a characterization tool allows one to evaluate the enhancement of the local field intensity in coupled nanoantennas as well as in single nanoparticles [35, 34].

The origin of TPL has been investigated in several recent studies [360, 407, 408]. By comparing TPL emission and linear scattering spectra from gold gap antennas, a clear correlation between the linear and nonlinear response of the sample has been determined, providing a recipe to enhance and spectrally reshape the TPL spectrum using LSP resonances [409]. A following study shows how luminescence features information cross-polarized to the excitation light, with an intensity corresponding to the density of states of the transversal modes of the nanoantenna, thus suggesting that luminescence is not necessarily a polarization conserving phenomenon as discussed in the previous section [410].

TPL microscopy evolved into a powerful tool to monitor the local density of states in plasmonic antennas [411]. Spatially resolved mode mapping of individual and coupled gold nanowires, for example, has been performed using TPL microscopy, thus directly visualizing the evolution of the modal field as a function of the excitation wavelength both in the gap and along the nanowires forming the antenna [412]. The same approach has also been used to monitor the selective switching of hot-spots within complex coupled antenna architectures by means of spatially phase-shaped beams [413]. Finally, the antibonding mode of single crystalline symmetric dipole antennas, which exhibits a significantly lower near-field intensity enhancement compared to the bonding mode, can still dominate the TPL signal in the case of strong coupling [414].

## 8.5 Conclusions and outlook

This Chapter reviewed the main concepts and recent advances in the study of nonlinear optical antennas. New phenomena arise when the linear dependence between the polarization currents and the propagating light field breaks down.

The design of nonlinear antennas is based on the well-established field of nonlinear optics. However, localized surface plasmons boost the light-matter interaction strength both in the linear and nonlinear regime. Furthermore, the symmetry of the particle geometries provides a mean to engineer the nonlinear response and to enhance selected nonlinear processes. While the nonlinear response of bulk materials is determined by the symmetry of the crystal lattice, the nonlinear response of nanoscale structures is determined by both the symmetry of the lattice and the symmetry of the geometry.

Nonlinear antennas hold promise for optoelectronic applications such as on-chip frequency conversion, switching, and modulation. The field is still in its infancy, and it can be expected that exciting new concepts and applications will emerge in the near future.